CHEMISTRY
A EUROPEAN JOURNAL

DOI: 10.1002/chem.201000823

Tripodal Thiols as Ligands for Molecular Magnets: Very Strong Antiferromagnetic Exchange Interactions in Vanadium(III) Clusters

Luke J. Batchelor, Emma Fitzgerald, Joanna Wolowska, Joseph J. W. McDouall, and Eric J. L. McInnes*[a]

Abstract: The synthesis, structural and magnetic characterisation of $[V^{III}_3O(tmme)_2(diimine)_2Cl]$ [diimine = 2,2′-bipyridine (**1**) or 1,10-phenanthroline (**2**)] and $(HNEt_3)_2[V^{III}_4O(tmme)_4]$ (**3**) is reported, in which H_3tmme is tris(mercaptomethyl)ethane, $MeC(CH_2SH)_3$, the thiol analogue of the famous tripodal alcohol ligands typified by H_3thme [tris(hydroxymethyl)ethane, $MeC(CH_2OH)_3$]. Complexes **1** and **3** have "T-shaped" and square topologies, respectively, and the latter is centred on a rare example of a square-planar oxide. The tri-thiolate ligands bind the periphery of the clusters and provide such strong antiferromagnetic exchange pathways that in both cases only a single total spin state is occupied up to room temperature, in the absence of metal–metal bonding. Magnetic data, electronic structure calculations and electrochemical data are reported.

Keywords: magnetic properties · solvothermal synthesis · thiols · tripodal ligands · vanadium

Introduction

Tripodal tris-alcohols such as the archetypal tris(hydroxymethyl)ethane [H_3thme; $MeC(CH_2OH)_3$] have long been used to template cluster formation in polyoxometallate chemistry[1] and more recently in later transition-metal ion clusters,[2] particularly with a view to molecular magnets.[3] The ligand can be mono-, di- or tri-deprotonated such that several metal ions can be bound, and the trigonal disposition of the three alcohol/alkoxide arms tends to direct formation of triangular fragments.[1,2] These ligands have also been exploited to allow formation of reduced [vanadium(IV)] polyoxovanadates by reduction of charge density (compared to naked oxide clusters),[1,2] and we have recently extended this idea to lower-valent, vanandium(III) clusters.[4] In the context of molecular magnets the triangular arrangement of metal ions tends to lead to competing antiferromagnetic interactions, which in turn can lead to exciting magnetic behaviour.[3] In contrast, although the tris-mercapto analogue of H_3thme, tris(mercaptomethyl)ethane [H_3tmme; $MeC(CH_2SH)_3$], has been known[5] since the 1970s, its cluster chemistry is little explored. The notable exception is in Pickett's hydrogenase mimics in which H_3tmme and derivatives have been used to form low-valent Fe_xS_y-based clusters that are active in electrocatalytic hydrogen evolution.[6,7] We are now beginning to explore H_3tmme as a ligand for molecular magnets to investigate its potential for a) structure directing, as demonstrated for H_3thme; b) stabilizing lower-valent clusters, as exemplified by Pickett's work; and c) mediating much stronger exchange interactions than the equivalent O-donor ligands, leading to, for example, much better isolated spin ground states. Some potential advantages and disadvantages of this ligand in this context are hinted at by Pickett's work. For example, $[Fe_4(tmme)_2(CO)_8]$ has formal oxidation states $\{Fe^{II}_2Fe^{I}_2\}$, illustrating the stabilization of low-valent clusters, but is also diamagnetic because of the formation of metal–metal bonds.[6] We have chosen to start by investigating the cluster chemistry of H_3tmme with the vanadium(III) ion because we have already been exploring the equivalent chemistry with H_3thme,[4] and also because there is a substantial literature with simpler dithiolates,[8,9] particularly from the work of Christou,[8] initially inspired by the relevance to early transition-metal sulfide materials. Here we report our initial results with the surprising formation of molecules based on square cluster geometries ("T-shaped" and square), which are based on a single binding mode of

[a] L. J. Batchelor, E. Fitzgerald, Dr. J. Wolowska, Dr. J. J. W. McDouall, Prof. E. J. L. McInnes
School of Chemistry, The University of Manchester
Oxford Road, Manchester M13 9PL (UK)
Fax: (+44) 161-275-4616
E-mail: eric.mcinnes@manchester.ac.uk

Supporting information for this article is available on the WWW under http://dx.doi.org/10.1002/chem.201000823.

tmme^{3-}. We also report their magnetic and redox properties, supported by theoretical calculations to address the issue of potential metal–metal bonding that was a feature of the earlier V^{III}–thiolate work.

Results and Discussion

Synthesis, structural and electrochemical studies: Solvothermal and anerobic reaction of $[VCl_3(thf)_3]$ with 2,2′-bipyridine (bipy; 1:1) in MeCN at 100 °C, followed by addition of H_3tmme (2 equiv) and Et_3N and further heating at 150 °C gave deep-purple crystals of $[V^{III}{}_3O(tmme)_2(bipy)_2Cl]$ (**1**; Figure 1) in reasonable yield (23 %) directly on cooling to room temperature. The bipy can be readily replaced with other chelating diimines, for example, an analogous reaction with 1,10-phenanthroline (phen) gives $[V_3O(tmme)_2(phen)_2Cl]$ (**2**) in excellent yield (85 %).

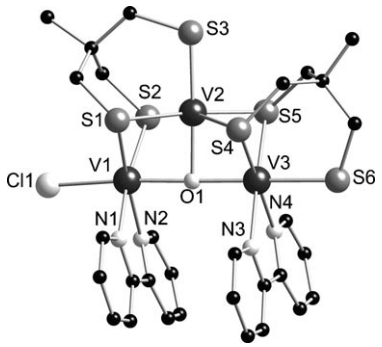

Figure 1. Crystal structure of **1** (C = black spheres, H atoms are omitted for clarity).

Complex **1** crystallises in $P\bar{1}$ (Table 1 and Table S1 in the Supporting Information). The molecule consists of three distorted-octahedral V^{III} ions arranged in a T-shape around a μ_3-oxide (O1). In the tri-metallic core V1 and V3 bridge through a linear V-O-V interaction [179.1(3)°], and V2 connects to V1 and V3 through right-angled V-O-V connections [88.19(18) and 90.96(19)°, respectively]. There are two triply deprotonated tmme^{3-} ligands, each with two μ_2-thiolate arms, one ligand bridging V2 to V1 the other bridging V2 to V3, and one terminally binding arm that binds *trans* to O1 in each case. The terminal thiolate arm of the tmme^{3-} that bridges V1 to V2 coordinates to V2. Hence, V2 has a $\{VOS_5\}$ coordination sphere. The terminal thiolate arm of the other tmme^{3-} coordinates to V3. V1 and V3 are both chelated by a molecule of bipy, and the remaining coordination site at V1 is occupied by a terminal chloride *trans* to O1. Hence, V3 and V1 have $\{VOS_3N_2\}$ and $\{VOS_2N_2Cl\}$ coordination spheres, respectively. V1, V2, V3, O1 and the terminal thiolates (S3, S6) and chloride are near planar with respect to one another, with the bridging thiolates sitting above and below the plane. Bond valence sum (BVS) analysis gives all three vanadium ions as V^{III} (mean valence sum 3.10), as also required by charge balancing, and is confirmed by the magnetic properties (see below).

Complex **1** is formed by a two-step solvothermal reaction. The first step, reaction of $[VCl_3(thf)_3]$ with bipy, forms *mer*-$[VCl_3(bipy)(MeCN)]$. We have previously ioslated this material and used it as a precursor for larger V^{III} clusters by reaction with H_3thme and analogues.[4a,b] Here, we have simply generated it in situ and treated it with H_3tmme and base. The incorporation of oxide in the structure of **1** is adventitious, presumably arising from water in the triethylamine, although attempts to dry this reagent made no significant difference to the reaction. If the reactions were performed without addition of Et_3N, deep-purple solutions were obtained from which we have been unable to isolate any crystalline products. Attempts to replace O1 with a μ_3-sulfide by including Li_2S in the reaction failed, giving only **1**.

The T-shaped $\{V_3O\}$ core and the binding pattern of the two tmme^{3-} ligands (two μ_2-arms and one terminal arm, in the same sense of rotation with respect to the $\{V_3O\}$ core) suggested that a complete $\{V_4O\}$ square should be isolable if the chelating bipyridine ligands could be replaced. Hence, we replaced bipy in the first stage of the reaction with a "poorer" ligand, 2-aminopyridine (ampy), which generally

Table 1. Crystal data for **1**–**3**.

	1	**2**	**3**
formula	$C_{31}H_{35.5}ClN_{4.5}OS_6V_3$	$C_{36}H_{37}ClN_5OS_6V_3$	$C_{36}H_{74}N_4OS_{12}V_4$
M_r	867.77	936.34	1167.47
crystal dimensions [mm]	0.4 × 0.1 × 0.05	0.4 × 0.4 × 0.4	0.4 × 0.2 × 0.1
crystal system	triclinic	monoclinic	triclinic
space group	$P\bar{1}$	$P2(1)/n$	$P\bar{1}$
a [Å]	14.0223(6)	9.7021(4)	10.7210(2)
b [Å]	16.2024(7)	12.6805(4)	11.8046(2)
c [Å]	17.2379(7)	31.3895(11)	20.6460(4)
α [°]	79.523(4)	90.000	102.090(2)
β [°]	88.898(3)	97.79(0)	93.342(2)
γ [°]	67.221(4)	90.000	96.462(2)
U [Å^3]	3545.0(3)	3826.1(2)	2529.68(8)
Z	4	4	2
ρ_{calcd}	1.626	1.625	1.533
T [K]	100	100	100
$2\theta_{max}$	23.26	26.37	30.51
data collected	14857	16005	34305
(unique reflns)	(9571)	(7732)	(15229)
no. of parameters	842	687	522
final $R1$, $wR2$	0.0551, 0.1208	0.0405, 0.0928	0.0351, 0.0836
[$I>2\sigma(I)$] (all data)	(0.11210, 0.1405)	(0.0608, 0.1003)	(0.0592, 0.1004)

binds terminally[10] although there is one example in which it chelates.[11]

Solvothermal reaction of $[VCl_3(thf)_3]$ with ampy (1:1) in MeCN at 100 °C gave a pink solution. We have not been able to isolate this intermediate, although given the common binding mode of ampy it is likely to be $[VCl_3(ampy)_2(MeCN)]$. Addition of H_3tmme (1.08 mmol) and Et_3N (3.24 mmol) to this pink solution, with further heating at 150 °C then cooling to room temperature, gave a deep-red solution. Dark-red crystals of $(HNEt_3)_2[V^{III}_4O(tmme)_4]$ (**3**, Figure 2) form after standing (in a glove box) for several days (overall yield 16%, based on $[VCl_3(thf)_3]$).

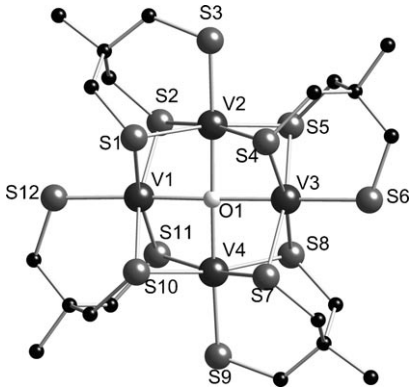

Figure 2. Crystal structure of the cluster anion $\mathbf{3}^{2-}$. The labelling scheme is the same as for Figure 1.

Complex **3** crystallises in $P\bar{1}$ (Table 1 and Table S1 in the Supporting Information) and is a salt. The $\mathbf{3}^{2-}$ cluster anion contains four distorted-octahedral V^{III} ions centred on a μ_4-oxide (O1), which lies in the $\{V_4\}$ plane [V1-O1-V3 and V2-O1 V4 176.82(8) and 178.84(9)°, respectively], thus forming the targeted $\{V_4O\}$ square. Although there is precedent for square-planar geometry for oxides in molecular species, examples are rare.[8d,12] Four triply deprotonated $tmme^{3-}$ ligands bind in the same manner as in **1**, and all in the same sense such that they are related by a pseudo four-fold axis. Hence, $\mathbf{3}^{2-}$ has pseudo-C_4 point symmetry. All metal ions are V^{III} as determined by BVS (mean valence sum 3.12, which is also consistent with the magnetic data) with the charge balance being provided by two $HNEt_3^+$ cations.

It is instructive to compare the chemistry that leads to **1**–**3** with equivalent reactions that use H_3thme. Solvothermal reaction of $[VCl_3(thf)_3]$ with bipy, to form *mer*-$[VCl_3(bipy)(MeCN)]$, then with H_3thme gives $[V^{III}_4(thme)_2(bipy)_3Cl_6]$ (**4**; Scheme S1 in the Supporting Information).[4b] The structure of **4** is a $\{V_4\}$-centred triangle, in which both $thme^{3-}$ ligands cap the central metal ion and each alkoxide arm forms μ_2-bridges to one of the peripheral metal ions. The molecule has pseudo-C_3 point symmetry. A similar reaction by using pyridine instead of bipy (allowing larger cluster growth, as argued above) gives the hexametallate structure $[V^{III}_6O(thme)_4Cl_6]^{2-}$ ($\mathbf{5}^{2-}$; Scheme S1 in the Supporting Information), in which a $\{V_6\}$ octahedron is centred on a μ_6-oxide.[4c] The four $thme^{3-}$ ligands in $\mathbf{5}^{2-}$ cap alternate $\{V_3\}$ faces of the $\{V_6\}$ octahedron (each arm μ_2-binding) to give pseudo-T_d point symmetry. It could be argued that the $\{V_4O\}$ core of $\mathbf{3}^{2-}$ is a fragment of this structure. However, this ignores the very different binding mode of the tripodal ligand, which would not allow completion of the $\{V_6\}$ octahedron.

Hence, in these compounds $tmme^{3-}$ does not bridge as extensively as $thme^{3-}$. Each $thme^{3-}$ binds four (μ_2,μ_2,μ_2-binding mode, or 4.222 in Harris notation)[13] or three (μ_2,μ_2,μ_2- or 3.222) metal ions in **4** and $\mathbf{5}^{2-}$, respectively. Each $tmme^{3-}$ binds two metal ions (μ_2,μ_2,μ_1- or 2.221) in **1** and $\mathbf{3}^{2-}$. This leads to the square-based, rather than trigonal-based, cluster topologies.

In the dithiolate chemistry of Christou[8] and others,[9] the most common bridging mode for the dianion of 1,2-ethanedithiol (H_2edt) is a simple μ_2,μ_2 (2.22 in Harris notation), although it often also acts as a simple chelate.[8,9] This bridging mode has some similarity to that of $tmme^{3-}$ observed in this work, in which the third arm acts as a simple terminal ligand. In fact $\mathbf{3}^{2-}$ has a close precedent in $[V_4O(edt)_2Cl_8]^{2-}$, formed from reaction of VCl_3 with Na_2edt.[8d] In this species, two opposite edges of a $\{V_4\}$ square are bridged by μ_2,μ_2-edt^{2-} with the other edges both bridged by two μ_2-Cl^-, and each V^{III} ion has a terminal chloride.

Complexes **1**–**3** oxidise readily on exposure to air. Cyclic voltammetry studies on **2** (which is more soluble than **1**) in CH_2Cl_2 solution reveal a reversible one-electron oxidation at −0.05 V vs. Ag/AgCl, whereas $\mathbf{3}^{2-}$ undergoes reversible oxidation at −0.43, −0.01 and +0.61 V in the available potential window (Figure S1 in the Supporting Information). It seems likely that this redox activity is associated with the $\{VS_5O\}$ centres. Attempts to chemically isolate the oxidation products have not been successful to date.

Magnetic studies: χT for **1** (χ is the molar magnetic susceptibility) is much lower than the value calculated for three independent V^{III} ($s=1$) ions (Figure 3). It varies little on cooling between 300 and 20 K, ranging from 1.4 to

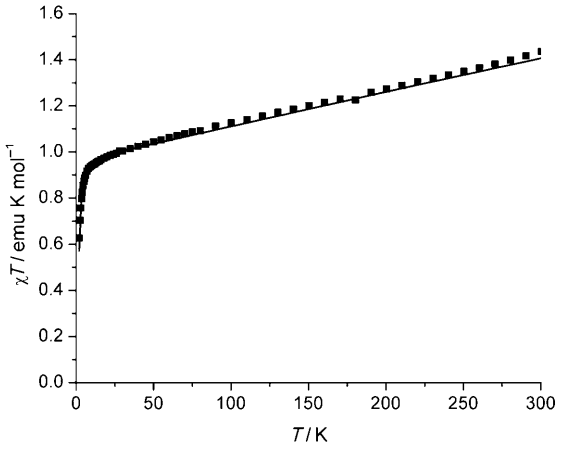

Figure 3. A plot of $\chi T(T)$ for **1** measured in an 0.5 T applied magnetic field (■); calculated curve for the parameters in the text (——).

1.0 emu K mol^{-1}. This variation is linear, which is indicative of a significant temperature-independent paramagnetism (TIP) contribution[14] rather than of depopulation of excited spin states. A linear fit to the 300–50 K data gives $\chi_{TIP} = 0.5 \times 10^{-3}$ emu mol^{-1} per metal ion, which is in the range found for many vanadium materials.[8ef,15] Correcting for this[16] gives an essentially temperature-independent (down to ca. 20 K) χT value of 0.95 emu K mol^{-1}, which implies a spin triplet. This is consistent with magnetisation (M) versus applied magnetic field (H) data (tending to saturation at 2 μ_B; Figure 4). Below 10 K, χT collapses owing to zero-field splitting (zfs) effects within the triplet (see below).

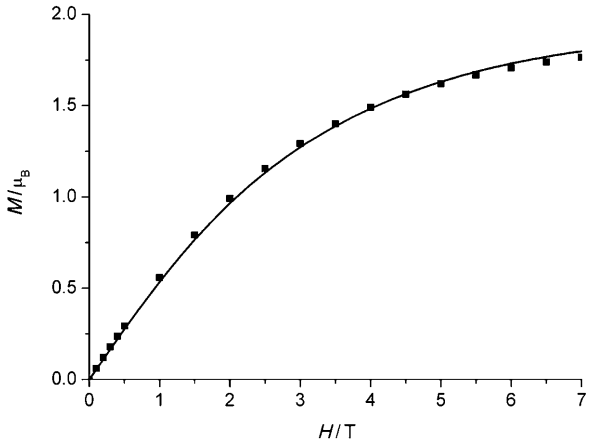

Figure 4. A plot of M(H) for **1** measured at 2 K (■); calculated curve by using the parameters in the text (——).

The magnetic response of the tetrametallic **3** is diamagnetic from 300 to 27 K (in a 5 kG applied field), which is consistent with a spin singlet. At lower temperatures a weak paramagnetic signal is observed that is smaller in magnitude than the diamagnetic contributions of the sample and holder. This is presumably due to a paramagnetic impurity (both **1** and **3** are very air sensitive).

The magnetic behaviour of both **1** and **3** are consistent with essentially exclusive population of only a single spin state up to room temperature in each case, implying very strong antiferromagnetic (AF) exchange coupling between the V^{III} ions.

Metal–metal bonding has been implicated in a number of thiolate-bridged species. For example, $[V^{III}_2(edt)_4]^{2-}$ (two bridging edt^{2-}; V–V 2.60 Å)[9] and $[V^{III}_2O(SPh)_4(Me_2bipy)_2]$ (V–V 2.58 Å)[8e] are both proposed to have V–V single bonds. This "ties up" one electron each from the d^2 ions and the magnetic data were modelled as simple $s = {}^1/_2$ dimers in both cases with $J < -350$ cm^{-1}.[8e,f] However, because $|J|$ is so large, identical fits with the same values could be obtained based on $s = 1$ dimer models (i.e., the fits only depended on the ground to first excited state gap). The presence of V–V bonding was supported by extended Hückel calculations.

The neighbouring *cis* metal ions in both **1** and $\mathbf{3}^{2-}$ have similar bridging arrangements to $[V^{III}_2O(SPh)_4(Me_2bipy)_2]$, namely, two thiolate ligands and an oxide. However, their V···V (*cis* at the oxide) distances (2.70 and 2.74 Å in **1**; 2.80-2.84 Å in $\mathbf{3}^{2-}$) are considerably longer and out of the range considered typical for a V^{III}–V^{III} bond. Hence, we have interpreted our magnetic data by assuming that there is no metal–metal bonding. We return to this subject in the computational studies section.

Complex **1** can then be approximated to the topology of an isosceles triangle, giving the spin Hamiltonian described in [Eq. (1)] with $s_1 = s_2 = s_3 = 1$.

$$\mathscr{H} = -2J_1(\hat{s}_1\hat{s}_3) - 2J_2(\hat{s}_1\hat{s}_2 + \hat{s}_2\hat{s}_3) + \sum_i g_i\mu_B\hat{s}_iB + (\sum_i D_i\hat{s}^2_{i,z}) \quad (1)$$

This allows two distinct possibilities for a well-isolated triplet ground state:

1) The $|0,1>$ triplet ($|S_{13},S>$, in which S is the total spin and S_{13} is the intermediate spin from coupling s_1 and s_3), resulting from strongly AF J_1 (linear through the oxide) and $|J_1| \gg |J_2|$. This state is localised on V2.
2) The $|2,1>$ triplet, resulting from strongly AF J_2 (through the thiolate bridges) with $|J_2| \gg |J_1|$. This state is localised on all three metal ions.

We have previously studied a related all-oxygen-bridged T-shaped V^{III} trimer $[V_3O(O_2CPh)_2(OEt)_2(bipy)_2Cl_3]$ and determined the analogous J_1 interaction to be -68 cm^{-1}.[4b] This is not nearly strong enough to account for the magnetic behaviour of **1** (i.e., insignificant excited-state population at 300 K) based on model 1, hence we favour model 2 in which the thiolate pathway dominates. Again, we discuss this further in the computational studies section.

The exchange part of the Hamiltonian in [Eq. (1)] can be solved by Kambé methods: this gives the separation between the $|2,1>$ ground state and the $|1,0>$ first excited state (a singlet) as $-2J_2+4J_1$. Because of the negligible excited-state population at all temperatures, we are restricted to estimating a lower limit for this energy gap. Furthermore, in order to estimate J_2 we must assume a value for J_1. Hence, we have fixed $J_1 = -70$ cm^{-1} from the value found for $[V_3O(O_2CPh)_2(OEt)_2(bipy)_2Cl_3]$, and have also fixed χ_{TIP} (see above) and $g = 1.96$. We find when $J_2 > -580$ cm^{-1}, the calculated curve starts to decrease with increasing temperature at high temperatures: this is due to population of the first excited spin state, which is diamagnetic. Hence, with these approximations, we find a lower limit for the strength of the strong AF interaction through two μ_2-thiolate arms of $tmme^{3-}$, $J_2 < -580$ cm^{-1}. The calculated $\chi T(T)$ curve for $J_2 = -580$ cm^{-1} is in Figure 3 [see Figure S2 in the Supporting Information for $\chi(T)$ and $\chi^{-1}(T)$]. These J values give a lower limit for the energy gap to the first excited state of 880 cm^{-1}, hence an upper limit to its population at 300 K of 0.5 %.

Modelling the $M(H)$ data and the low-temperature collapse in χT for **1** (Figure 3 and Figure 4) requires significant anisotropy in the ground state. This could be due to local zfs effects or, given the very large $|J_2|$, an anisotropic component of the exchange. We have chosen to model the data by inclusion of the local zfs terms that are described by the Hamiltonian in [Eq (1)]. For simplicity these were assumed to be axial and equal at each V^{III} site: this gives $D_{1-3}=5.2\,cm^{-1}$, which corresponds to a zfs in the $|2,1>$ ground state of $4.1\,cm^{-1}$. Clearly this is a simplistic argument, but a large anisotropy is consistent with W-band (95 GHz) EPR data (Figure S3 in the Supporting Information), which show that the zfs must be substantially greater than the microwave energy ($>3\,cm^{-1}$); higher frequency measurements would be necessary to determine this number precisely.

Extending the model for **1** to $\mathbf{3}^{2-}$, we have the exchange part of the spin given by the Hamiltonian in [Eq. (2)].

$$\mathscr{H} = -2J_1(\hat{s}_1\hat{s}_3 + \hat{s}_2\hat{s}_4) - 2J_2(\hat{s}_1\hat{s}_2 + \hat{s}_2\hat{s}_3 + \hat{s}_3\hat{s}_4 + \hat{s}_1\hat{s}_4) \qquad (2)$$

This can also be solved by Kambé methods and, by assuming $|J_2| \gg |J_1|$ as above, the ground state is the $|22,0>$ singlet ($|S_{13}S_{24},S>$), with the first excited state being the $|22,1>$ triplet at a relative energy of $-2J_2$ (note this is independent of J_1). If we assume the same lower bound for $|J_2|$ as for **1** (given the identical chemical arrangement), this gives an energy gap of at least $1160\,cm^{-1}$. This corresponds to a population of the lowest paramagnetic state of 1% at 300 K, consistent with the observed diamagnetism.

The $J_2 < -580\,cm^{-1}$ value estimated for **1** can be compared with $J=-419\,cm^{-1}$ reported for $(NEt_4)_2[V_2(edt)_4]$ (through two μ_2,μ_2-edt^{2-}) and $J=-355\,cm^{-1}$ reported for $[V^{III}{}_2O(SPh)_4(Me_2bipy)_2]$ (through two μ_2-thiolates and an oxide).[8e,f] The only magnetic data reported for $(NBu_4)_2[V_4O(edt)_2Cl_8]$ are Evans NMR measurements (CD_3CN solution), which give a magnetic moment of $2\,\mu_B$ per V^{III} ion[8d]. This is in stark contrast to our findings on **3**, and is presumably due to the much weaker exchange facilitated by the four μ_2-chloride bridges. The *cis* V···V distances in $[V_4O(edt)_2Cl_8]^{2-}$ (2.81–2.86 Å) are comparable to those in $\mathbf{3}^{2-}$. However, the triangular $[V^{III}{}_3(S)(S_2)_3(bipy)_3](PF_6)$ has V–V distances as long as 2.75 Å and is reported to be diamagnetic,[8e] and this was explained as being due to V–V bonding. Hence, in order to test our assumptions of the lack of V–V bonding, and on the identity of the ground states, we have performed electronic structure calculations on **1** and $\mathbf{3}^{2-}$.

Computational studies: To investigate the electronic structures of **1** and $\mathbf{3}^{2-}$ density functional calculations[17] by using the Def2-SVP basis sets[18] and the B3LYP exchange-correlation functional[19] were performed. Both systems yielded symmetry-broken solutions to the Kohn–Sham equations and hence all geometries were fully optimized, starting from the crystallographically determined structures, by using the spin-unrestricted formalism. All structures were confirmed as stationary minima by vibrational analysis. Based on the optimized geometries the lowest energy triplet ($S_z=1$) and singlet ($S_z=0$) states of **1** were calculated; the triplet was at significantly lower energy. Mayer bond-order analysis[20] of the triplet structure shows pronounced V–S interactions with bond orders for the sulphur atoms in the plane of the V_3 unit of 1.15 and 1.19 and those outside the V_3 plane ranging from 0.57–0.73. There are also significant V–O interactions with bond orders of 0.67 (V3), 0.50 (V2) and 0.82 (V1). However, there is very little indication of V–V bonding (maximum calculated bond order of 0.14). The calculated spin-density map for **1** shows the spins to be distributed equally over all three V^{III} centres (Figure 5), with the Mulliken spin densities being +2.08 (V3), −2.14 (V2) and +2.03 (V1). Thus the calculations support the coupling scheme 2 used above with dominant thiolate exchange pathways.

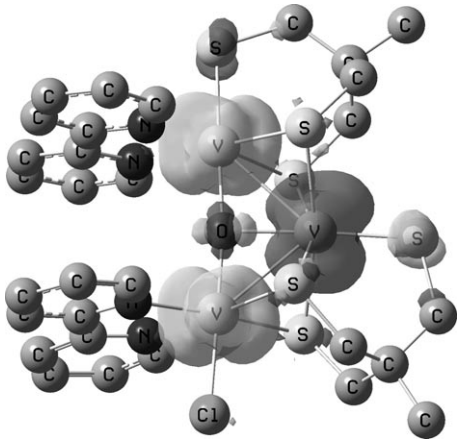

Figure 5. B3LYP/Def2-SVP spin density of the optimized triplet ($S_z=1$) structure of **1** (light shading indicates positive spin and dark shading represents negative spin).

Similar calculations for $\mathbf{3}^{2-}$ yield an equivalent picture; the optimized broken symmetry ($S_z=0$) ground state structure of $\mathbf{3}^{2-}$ and the corresponding spin density are shown in Figure 6. The vanadium ions show Mulliken spin densities of $|2.13|$ (alternating in sign on each atom). The V–S bonding appears similar with the in-plane sulfur atoms having bond orders (with the adjacent V atom) of 1.05, whereas the out-of-plane V–S bond orders range from 0.60–0.64. The V–O bond orders are essentially all 0.47. Once again the V–V bonding is negligible with a maximum bond order of 0.12.

Conclusion

In conclusion, $tmme^{3-}$ exhibits significantly different binding modes to its all-oxygen-donor analogues by not having the same tendency to template trigonal metal fragments. Nevertheless, this work shows that it is a promising ligand for future studies in molecular magnetism. In both **1** and **3** it gives AF exchange pathways, which are so strong that only a single spin state is populated up to room temperature. This is a desirable property for molecular nanomagnets in

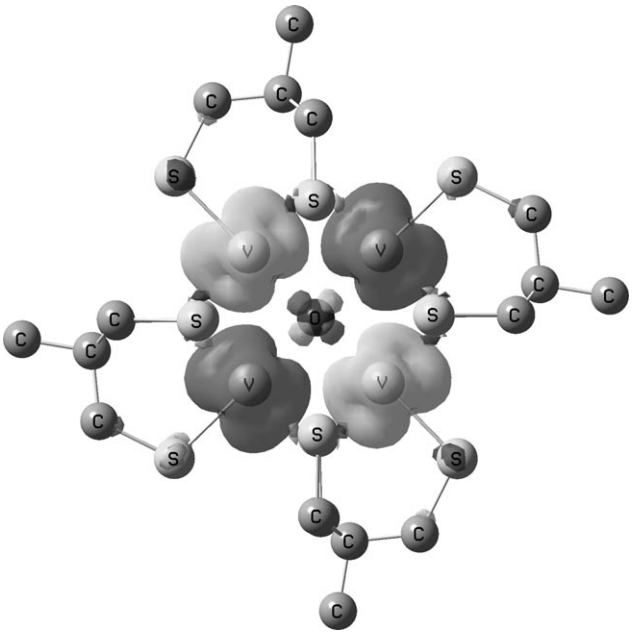

Figure 6. B3LYP/Def2-SVP spin density of the optimized singlet ($S_z=0$) structure of $\mathbf{3}^{2-}$ (light shading indicates positive spin and dark shading represents negative spin).

the context of both single-molecule magnet behaviour[24] and proposed applications in quantum information processing,[25] with consequences for relaxation mechanisms and lifetimes. An obvious target then is to prepare larger clusters with a ferrimagnetic-like spin structure (i.e., AF coupling between unequal sub-lattices) to give non-zero spin ground states, as with **1**. The reversible redox behaviour of **1** and $\mathbf{3}^{2-}$ at mild potentials is also an attractive feature because this could allow facile redox-switching between, for example, paramagnetic and diamagnetic states. Attempts to isolate the oxidation products of **1** and $\mathbf{3}^{2-}$ are ongoing.

Experimental Section

General: Solids **1**, **2** and **3** degrade in air and all manipulations, in synthesis, and magnetic and spectroscopic measurements, were performed under an inert atmosphere (dinitrogen-purged glove box and Schlenk line). All chemicals were purchased from Aldrich. Solvents were from BDH and were distilled before use. $[VCl_3(thf)_3]$[21] and H_3tmme[5a] were prepared by following reported procedures.

Synthesis of $[V_3O(tmme)_2(bpy)_2Cl]\cdot MeCN$ (1): A mixture of $[VCl_3(thf)_3]$ (0.200 g, 0.54 mmol) and bpy (0.084 mL, 0.54 mmol) in MeCN (8 mL) was heated in a Teflon-lined autoclave at 100 °C for 12 h under autogenous pressure, then cooled to room temperature. H_3tmme (0.155 mL, 1.07 mmol) and Et_3N (0.443 mL, 3.21 mmol) were added to the mixture, which was heated in the Teflon-lined autoclave at 150 °C for a further 12 h. Cooling to room temperature (0.05 °C min^{-1}) gave deep-purple crystals of **1**, which were washed with MeCN and Et_2O. Yield: 36 mg, 23 %; IR (Nujol): $\tilde{\nu}=1634$ (m), 1597 (s), 1471 (m), 1441 (s), 1408 (w), 1384 (w), 1312 (m), 1293 (m), 1246 (m), 1155 (m), 1113 (w), 1058 (w), 1042(m), 1026 (m), 910 (w), 873 (w), 812 (w), 768 (s), 734 (m), 671 (w), 654 (w), 636 (w), 526 (m), 481 (w), 441 (w), 416 cm^{-1} (m); elemental analysis calcd (%) for $V_3C_{32}H_{37}N_5OS_6Cl$: C 43.26, H 4.19, N 7.88, Cl 3.99, S 21.65; found: C 43.18, H 4.01, N 7.37, Cl 4.07, S 21.73.

Synthesis of $[V_3O(tmme)_2(phen)_2Cl]\cdot MeCN$ (2): A similar reaction as for **1**, but substituting phen (0.096 g, 0.54 mmol) for bpy, gave deep-purple crystals of **2**. Yield: 143 mg, 85 %; IR (Nujol): $\tilde{\nu}=1634$ (w), 1624 (w), 1509 (m), 1450 (w), 1421 (m), 1376 (w), 1313 (m), 1298 (m), 1244 (s), 1194 (m), 1135 (m), 984 (m), 868 (w), 852 (w), 839 (m), 808 (w), 780 (w), 766 (w), 744 (w), 721 (s), 670 (w), 645 (m), 627 (w), 534 (m), 497 (w), 441 (w), 426 (w), 408 cm^{-1} (w); elemental analysis calcd (%) for $V_3C_{36}H_{37}N_5OS_6Cl$: C 46.18, H 3.98, N 7.47, Cl 3.78, S 20.54; found: C 46.36, H 3.84, N 7.23, Cl 3.06, S 20.23.

Synthesis of $[HEt_3N]_2[V_4O(tmme)_4]\cdot 2MeCN$ (3): A mixture of $[VCl_3(thf)_3]$ (0.200 g, 0.54 mmol) and ampy (0.050 mL, 0.54 mmol) in MeCN (8 mL) was heated in a Teflon-lined autoclave at 100 °C for 12 h then cooled to room temperature. H_3tmme (0.155 mL, 1.07 mmol) and Et_3N (0.443 mL, 3.21 mmol) were added to the mixture, which was heated further at 150 °C for 12 h. Cooling the solution to room temperature (0.05 °C min^{-1}) gave a deep-red solution. Slow evaporation of this solution (in a glove box) gave dark-red crystals of **3**, which were washed with a small amount of MeCN followed by Et_2O. Yield: 25 mg, 16 %; IR (Nujol): $\tilde{\nu}=$ 1462 (m), 1432 (w), 1406 (m),1366 (m), 1287 (s), 1247 (m), 1154 (w), 1111 (m), 1058 (w), 1037 (w), 1012 (m), 917 (w), 874 (m), 861 (w), 831 (w), 813 (m), 719 (m), 576 (s), 479 (m), 413 cm^{-1} (m); elemental analysis calcd (%) for $V_4C_{36}H_{74}N_4OS_{12}$: C 37.03, H 6.38, N 4.79, S 32.90; found: C 36.88, H 6.43, N 4.73, S 31.81.

Physical measurements: Magnetic data were measured on powdered samples in 1, 0.5 and 0.1 T applied magnetic fields on a Quantum Design XL7 SQUID magnetometer. Data were corrected for the diamagnetism of the sample holder and the sample (Pascal's constants). Modelling of magnetic data was by matrix-diagonalization methods by using MAGPACK software.[22] W-band EPR spectra were measured on a Bruker E500 CW spectrometer. Cyclic voltammetry measurements were performed on an Autolab PGSTAT30 potentiostat with an Ag/AgCl reference electrode, glassy carbon working electrode and a Pt wire auxiliary electrode. $E_{1/2}$ values are referenced to the Ag/AgCl electrode, on which the ferrocinium/ferrocene couple was measured at 0.46 V.

X-ray crystallography: Single-crystal X-ray diffraction data were measured on an Oxford Diffraction Xcaliber2 Bruker APEX II CCD diffractometer. Structure solution and refinement were performed by using SHELXTL.[23] The structures were refined by direct methods. Refinement of F^2 was against all reflections. All of the structures required substantial work to model disorder, although primarily this was limited to the solvent molecules, which were restrained appropriately. Crystallographic disorder in the structure of **4.2** required that both $tmme^{3-}$ ligands and the chloride ligand were split entirely over two sites. Displacement and geometric restraints were applied to the thermal parameters of these atoms. All H atoms were added geometrically except for the H atoms on the protonated amine in **4.3**. CCDC-771566 (**1**), 771567 (**2**) and 771568 (**3**) contain the supplementary crystallographic data for this paper. These data can be obtained free of charge from The Cambridge Crystallographic Data Centre via www.ccdc.cam.ac.uk/data_request/cif.

Acknowledgements

We are grateful to the EPSRC(UK), including for the National Service for Multi-Frequency EPR, and the EC (MagMaNet NoE) for funding. We also thank the referees for helpful comments.

[1] a) M. I. Khan, J. Zubieta, *Prog. Inorg. Chem.* **1995**, *43*, 1; b) A. Müller, J. Meyer, H. Bogge, A. Stammler, A. Botar, *Chem. Eur. J.* **1998**, *4*, 1388.

[2] K. Hegetschweiler, H. Schmalle, H. M. Streit, W. Schneider, *Inorg. Chem.* **1990**, *29*, 3625.

[3] a) A. Cornia, D. Gatteschi, K. Hegetschweiler, L. Hausherr-Primo, V. Gramlich, *Inorg. Chem.* **1996**, *35*, 4414; b) A. Cornia, A. C. Fabretti, P. Garrisi, C. Mortalò, D. Bonacchi, D. Gatteschi, R. Sessoli, L. Sorace, W. Wernsdorfer, A-L. Barra, *Angew. Chem.* **2004**, *116*, 1156;

Angew. Chem. Int. Ed. **2004**, *43*, 1136; c) E. K. Brechin, *Chem. Commun.* **2005**, 514; d) R. Shaw, I. S. Tidmarsh, R. H. Laye, B. Breeze, M. Helliwell, E. K. Brechin, S. L. Heath, M. Murrie, S. Ochsenbein, H-U. Güdel, E. J. L. McInnes, *Chem. Commun.* **2004**, 1418.

[4] a) I. S. Tidmarsh, E. Scales, P. R. Brearley, J. Wolowska, L. Sorace, A. Caneschi, R. H. Laye, E. J. L. McInnes, *Inorg. Chem.* **2007**, *46*, 9743; b) I. S. Tidmarsh, J. J. Batchelor, E. Scales, R. H. Laye, L. Sorace, A. Caneschi, J. Schnack, E. J. L. McInnes, *Dalton Trans.* **2009**, 9402; c) L. J. Batchelor, R. Shaw, S. J. Markey, M. Helliwell, E. J. L. McInnes, *Chem. Eur. J.* **2010**, *16*, 5554.

[5] a) G. R. Franzen, G. Binsch, *J. Am. Chem. Soc.* **1973**, *95*, 175; b) C. Kolomyjec, J. Whelan, B. Bosnich, *Inorg. Chem.* **1983**, *22*, 2343.

[6] C. Tard, X. Liu, D. L. Hughes, C. J. Pickett, *Chem. Commun.* **2005**, 133.

[7] C. Tard, X. Liu, S. K. Ibrahim, M. Bruschi, L. de Gioia, S. C. Davies, X. Yang, L-S. Wang, G. Sawyers, C. J. Pickett, *Nature* **2005**, *433*, 610.

[8] a) R. W. Wiggins, J. C. Huffman, G. Christou, *Chem. Commun.* **1983**, 1313; b) J. K. Money, J. C. Huffman, G. Christou, *J. Am. Chem. Soc.* **1987**, *109*, 2210; c) J. K. Money, J. C. Huffman, G. Christou, *Inorg. Chem.* **1988**, *27*, 507; d) J. R. Rambo, J. C. Huffman, G. Christou, *J. Am. Chem. Soc.* **1989**, *111*, 8027; e) N. S. Dean, K. Folting, E. Lobkovsky, G. Christou, *Angew. Chem.* **1993**, *105*, 623; *Angew. Chem. Int. Ed. Engl.* **1993**, *32*, 594; f) N. S. Dean, S. L. Bartley, W. E. Streib, E. B. Lobovsky, G. Christou, *Inorg. Chem.* **1995**, *34*, 1608; g) J. R. Rambo, S. L. Castro, K. Folting, S. L. Bartley, R. A. Heinz, G. Christou, *Inorg. Chem.* **1996**, *35*, 6844.

[9] a) J. R. Dorfman, R. H. Holm, *Inorg. Chem.* **1983**, *22*, 3179; b) D. Szeymies, B. Krebs, G. Henkel, *Angew. Chem.* **1983**, *95*, 903; *Angew. Chem. Int. Ed. Engl.* **1983**, *22*, 885.

[10] a) M. F. Summers, P. J. Toscano, N. Bresciani-Pahor, G. Nardin, L. Randaccio, L. G. Marzilli, *J. Am. Chem. Soc.* **1983**, *105*, 6259; b) J. M. Casas, B. E. Diosdado, J. Fornies, A. Martin, A. J. Rueda, A. G. Orpen, *Inorg. Chem.* **2008**, *47*, 8767.

[11] C. M. Standfest-Hauser, K. Mereiter, R. Schmid, K. Kirchner, *Dalton Trans.* **2003**, 2329.

[12] V. S. Nair, K. S. Hagen, *Inorg. Chem.* **1994**, *33*, 185.

[13] $[X.Y_1Y_2Y_3\ldots]$ in which X is the total number of metal ions bound by the ligand, and the Y values refer to the number of metal ions attached to each donor atom, see: R. A. Coxall, S. G. Harris, D. K. Henderson, S. Parsons, P. A. Tasker, R. E. P. Winpenny, *Dalton Trans.* **2000**, 2349.

[14] O. Kahn, *Molecular Magnetism*, Wiley-VCH, Weinheim, **1993**.

[15] a) A. T. Casey, R. J. H. Clark, *Inorg. Chem.* **1968**, *7*, 1598; b) S. L. Castro, W. E. Streib, J. -S. Sun, G. Christou, *Inorg. Chem.* **1996**, *35*, 4462; c) C. Aronica, G. Chastanet, E. Zueva, S. A. Borshch, J. M. Clemente-Juan, D. Luneau, *J. Am. Chem. Soc.* **2008**, *130*, 2365, and references therein.

[16] Clearly there is a play-off between the diamagnetic correction applied and the value for TIP determined. The former has been measured for the sample holder and estimated from Pascal′s constants for the sample. Minor deviations from these values do not significantly affect the determined J values.

[17] Gaussian 03, Revision D.02, M. J. Frisch, G. W. Trucks, H. B. Schlegel, G. E. Scuseria, M. A. Robb, J. R. Cheeseman, J. A. Montgomery, Jr., T. Vreven, K. N. Kudin, J. C. Burant, J. M. Millam, S. S. Iyengar, J. Tomasi, V. Barone, B. Mennucci, M. Cossi, G. Scalmani, N. Rega, G. A. Petersson, H. Nakatsuji, M. Hada, M. Ehara, K. Toyota, R. Fukuda, J. Hasegawa, M. Ishida, T. Nakajima, Y. Honda, O. Kitao, H. Nakai, M. Klene, X. Li, J. E. Knox, H. P. Hratchian, J. B. Cross, V. Bakken, C. Adamo, J. Jaramillo, R. Gomperts, R. E. Stratmann, O. Yazyev, A. J. Austin, R. Cammi, C. Pomelli, J. W. Ochterski, P. Y. Ayala, K. Morokuma, G. A. Voth, P. Salvador, J. J. Dannenberg, V. G. Zakrzewski, S. Dapprich, A. D. Daniels, M. C. Strain, O. Farkas, D. K. Malick, A. D. Rabuck, K. Raghavachari, J. B. Foresman, J. V. Ortiz, Q. Cui, A. G. Baboul, S. Clifford, J. Cioslowski, B. B. Stefanov, G. Liu, A. Liashenko, P. Piskorz, I. Komaromi, R. L. Martin, D. J. Fox, T. Keith, M. A. Al-Laham, C. Y. Peng, A. Nanayakkara, M. Challacombe, P. M. W. Gill, B. Johnson, W. Chen, M. W. Wong, C. Gonzalez, J. A. Pople, Gaussian, Inc., Wallingford CT, **2004**.

[18] F. Weigend, R. Ahlrichs, *Phys. Chem. Chem. Phys.* **2005**, *7*, 3297.

[19] A. D. Becke, *J. Chem. Phys.* **1993**, *98*, 5648.

[20] The Mayer bond orders were calculated with in-house software based on: I. Mayer, *Int. J. Quantum Chem.* **1984**, *26*, 151 (closed shell); I. Mayer, *J. Comput. Chem.* **2007**, *28*, 204 (open shell).

[21] L. E. Manxzer, *Inorg. Synth.* **1982**, *21*, 135.

[22] J. J. Borrás-Almenar, J. M. Clemente-Juan, E. Coronado, B. S. Tsukerblat, *J. Comput. Chem.* **2001**, *22*, 985.

[23] SHELX-PC Package, Bruker Analytical X-ray Systems, Madison, WI, **1998**.

[24] D. Gatteschi, R. Sessoli, R. Villain, *Molecular Nanomagnets*, OUP, Oxford **2006**.

[25] A. Ardavan, O. Rival, J. J. L. Morton, S. J. Blundell, A. M. Tyryshkin, G. A. Timco, R. E. P. Winpenny, *Phys. Rev. Lett.* **2007**, *98*, 057201.

Received: April 1, 2010
Published online: August 2, 2010

